NORDIC VOLCANOLOGICAL INSTITUTE 78 04
UNIVERSITY OF ICELAND

THE INTERACTION BETWEEN VOLCANIC GASES AND SOLID TEPHRA

Notes on fluorine adhering to tephra of the 1970 Hekla eruption

by

Níels Óskarsson

February 1978

THE INTERACTION BETWEEN VOLCANIC GASES AND SOLID TEPHRA

Notes on fluorine adhering to tephra of the 1970 Hekla eruption

ABSTRACT

The mass distribution and sorting of tephra produced in the plinian phase of the 1970 Hekla eruption was controlled by the particle size distribution and height of the eruption column, and velocity of transport. In the vicinity of the volcano the mass distribution of soluble fluorine is controlled by particle size of the deposits but approaches the mass distribution of the tephra at longer distances. Deposition of soluble fluorine reaches maximum at a distance from the volcano determined by the velocity of the transporting medium.

SEM studies show the soluble fluorine to be chemically adsorbed on the surface of tephra particles. The adsorption is shown by experiment to occur at temperatures below 600°C in the cooling eruption column. Evaluation of reactions in the eruption column leads to the conclusion that formation of water soluble compounds adhering to tephra is principally controlled by environmental factors and to a lesser degree by the composition of the volcanic gas phase.

INTRODUCTION

Mt. Hekla is a central volcano on the western border of the South Eastern volcanic zone of Iceland (Sigvaldason, 1974). The mountain is a volcanic ridge (N´60°A, 1447 masl.) on a basement of late pleistocene hyaloclastite ridges formed in subglacial eruptions.

The postglacial eruptions of Hekla occur on a 6 km long fissure along the volcanic ridge. The products are icelandites to dacite.

The historic activity of Hekla is by far the best known among Icelandic volcanoes, due to the comprehensive work of Thorarinsson (1967) based on studies of tephra layers, historical records and observations of the 1947 eruption.

The first eruption of Hekla in historic times was a large plinian eruption of dacitic tephra in 1104 A.D. Since then major eruptions have occurred with 60 yrs. average interval, the last of these in 1947 lasting 13 months. The 1970 eruption was among the smallest Hekla eruptions recorded occurring after a repose of only 22 yrs., second shortest in historical times.

Thorarinsson´s (1967) studies have lead to the generalized description of an eruption of Hekla outlined below.

Following short (1-2 hours) seismic activity the eruptions start with a plinian phase of short duration (few hours), as reflected by the well defined tephra layers formed. The plinian phase grades through a vigorous fountaining activity to lava emission. At the onset of major eruptions the entire fissure of the volcanic ridge is active. As an eruption grades from the plinian activity, lava flow becomes more confined to individual craters on the fissure. The summit crater of Hekla is probably the vent of the major plinian columns, but lava seems to flow to a larger extent from craters at lower elevation. The tephra formed in major eruptions shows compositional gradation from dacite in the initial phase towards the composition of the subsequently produced lava, in most cases icelandites. The amount of acid material produced depends upon the repose between eruptions (Thorarinsson, 1967; Sigvaldason, 1974).

During the relatively small eruption of May 5th 1970 only parasitic craters at the South and North ends of the volcanic ridge were active. Tephra was ejected for two hours from the southern craters followed by lava flow for three days. At the northern end of the Hekla ridge a few craters produced lava the following two months. Acid pumice was ejected in minor amounts and the compositional gradation of the tephra is insignificant. The total lava production in the eruption is estimated by Thorarinsson (1970) to 0.2 km^3, as compared to 0.8 km^3 produced in 1947.

The historic eruptions of Hekla have been destructive not only by heavy tephra fall in populated areas but also by lethal fluorosis in grazing animals, even in areas outside the major deposits of tephra.

In this paper the mass distribution of tephra and mode of eruption will be related to the distribution of water soluble fluorine.

The chemistry of the soluble fluorine studied by leaching experiments, adsorption experiment and SEM technics will be reported. Finally the adsorption of soluble compounds on tephra in general will be discussed in relation to type and behaviour of volcanic eruptions.

The chemistry and proportions of soluble compounds adhering to tephra are found to be controlled by mode of eruption and environmental factors as well as by the composition of the volcanic gas phase.

MASS DISTRIBUTION OF THE TEPHRA

During the two first hours of the eruption a high plinian eruption column at the south end of the 6 km long fissure system of the volcano rose to 16 km height. Tephra was transported by strong wind to the NNW at a velocity of 20.6 m/s and deposited on a narrow sector (Fig. 1). At the northern end of the fissure system a second small eruption column gave rise to a small sector of deposits totally masked by the larger one beyond 15 km away from the volcano.

Thorarinsson (1970) points out that some acid pumice was produced mainly in the initial phase of the eruption. This must have happened before the rise of the plinian column since the bulk chemical composition of the tephra beyond 16 km from the volcano is uniform throughout the deposits and identical with the composition of lava reported by Thorarinsson & Sigvaldason (1972) and Sigvaldason (1974). The tephra particles are icelandite glass with occasional feldspar laths (Plate 1b).

The margins of the tephra layer are shown by the dotted line of Fig. 1. Its assymmetrical shape is explained by a northerly breeze at low elevation over the north coast during deposition (Thorarinsson, 1970).

The density distribution of the deposits is shown by dashed lines on Fig. 1. The map is based on samples collected from a known areal during deposition at locations marked with filled circles in the figure and extimations from the isopach map of Thorarinsson (1970).

To simplify calculations the AMT (axis of maximum thickness) is assumed to be a straight line and tephra is assumed to be deposited symmetrically around it.

The density (kg/m^2) of the deposits as a function of distance along the AMT is shown by curve A Fig. 2. Density sections transversal to the AMT were constructed (Fig. 2) and combined with curve A to give the mass distribution curve, B (kg/m) on Fig. 2. Total mass of the tephra is estimated to $4.3 \cdot 10^{10}$ kg by graphical integration of curve B.

Both density (kg/m^2) of the deposits and mass (kg/m) decreased reciprocially away from the volcano. This reflects the mass relations of tephra transport and the mass profile of the eruption column itself.

Even the simplest tephra deposits displayed by nature can hardly, if ever, be described by exact models. Many of the factors governing their deposition can, however, be evaluated by particle size analysis of the tephra.

PARTICLE SIZE DISTRIBUTION OF THE TEPHRA

Sheridan (1971) suggests three energy environments of tephra transport, fallout, suspended load and base load, each associated with single mode particle size distribution. Base load, although probably responsible for modification of the size distribution of the finest particles of a plinian tephra, will not be considered further in this text. Since the transportation of tephra is a sorting mechanism the fallout becomes better sorted the longer the distance travelled.

Suspended load, defined as particles following the turbulent motion of the transporting air mass contains the finest particles of the eruption column. A smooth gradation exists between fallout and suspended load, since the terminal velocity of a particle falling in air converges towards zero as its dimensions and density decreases. The expansion of an eruption column at height due to warming up of admixed air and decreasing atmospheric pressure result in radial dispersion of the suspended load. The fraction of suspended load is thus expected to increase towards the margins of tephra deposits.

Particle size distribution pattern of the Hekla 1970 tephra points toward fallout as the major mode of transportation.

Typical particle size cumulative curves of tephra are shown on Fig. 3. Samples from the southern lowlands (T04, T05, T43) show slightly bimodal particle size distribution probably due to single energy environment of transport from the two eruption columns, the lower being responsible for the shift towards finer particles. At the north coast the samples (T23, T31) show well sorted single mode size distribution indicating that the products of the lower eruption column are becoming a negligible small fraction of the total mass. The marginal samples (T29, T35) contain high amount of fines, probably due to transition towards suspended load, shown by the flattening of the cumulative curves towards finer particles. This trend is also visible in the curves T04 and T43 from the southern lowlands.

The particle size distribution of the sample T00 collected 16 km away from the volcano, probably reflects the size distribution of the coarse particles of the eruption column. The distance travelled in the fallout mode of transport is too short to permit effective sorting of the tephra. The discontinuity of the cumulative curve at 98 Wt. per cent reflects the contribution of the smaller eruption column.

ON THE ORIGIN OF A TEPHRA SAMPLE

The interpretation of the chemistry of soluble compounds adhering to tephra have to be based on understanding of the origin of a tephra sample. Although the dynamics of tephra transport are beyond the scope of this text the basic parameters governing transport and deposition of tephra will be reviewed and a simple model of its origin and particle size distribution derived.

The particle population of a tephra sample is derived from the particle population of the eruption column by selective transport mechanism. The distance travelled by a particle is determined by its initial elevation in the column, the velocity of transport and rate of fall (Walker et al., 1971). The largest particles of a tephra sample are derived from the highest elevation, since terminal velocity increases as a function of mass. All other particles are thus derived from successively lower elevations.

The particle size distribution of an eruption column is a key to the origin of a tephra sample. The first question which arises along with the column is whether its particle size distribution is even through all elevations during its rise. Wilson (1976) showed that a gravitational settling should occur in a plinian column. The magnitude of this fractionation is, however, hard to evaluate analytically. Another way of solving the problem is to reconstruct an eruption column from particle size distribution data.

The size and density of a tephra particle can be used to estimate its terminal velocity (Walker et al., 1971). Using the observed velocity of transport (20.6 m/s) and measured density (kg/m^3) of the Hekla 1970 tephra the trajectories of the mean and maximum sized particles of four samples were reconstructed in order to estimate their initial elevation in the eruption column. The sampling localities are shown on Fig.1 (T00, T04, T23, T31).

The computed elevation of the maxiumum and mean sized particles and their distance from the volcano are shown in Table I.

The average maximum elevation of 13.5 km is in good agreement with the observed absolute maximum elevation of 16 km. It will be noted that the computed elevation for the mean particle size of the bimodally sorted sample T04 is significantly low as compared to the others. This is probably reflecting the contribution of fines from the lower eruption column.

From Table I it is concluded that the largest particles along the entire deposits are derived from the maximum elevation of the eruption column and further that the mean particle size along the entire deposits is derived from another fixed elevation.

On Fig. 4 the mean particle size (curve A), maximum particle size (curve B) and average particle density of the Hekla 1970 tephra is shown as a function of distance from the volcano. The strong correlation between curves A and B supports the idea that gravitational sorting in the eruption column during its rise is not a factor controlling the particle size distribution of the tephra deposited away from it.

Sparks & Wilson (1976) studied the particle size distribution of a plinian eruption column. Their result is shown by curve A, Fig. 3, as a cumulative particle size distribution. From their data and the observations described above the following model for the origin of a tephra sample and its particle size distribution emerges.

The whole particle population of an eruption column is transported by an air mass. All particles below fixed dimensions are suspended in the air mass. At a fixed distance from the column all particles above fixed dimensions have reached the ground. The tephra available for deposition is thus the particle population between a fixed particle size (suspended load) and a particle size (maximum particle size) variable along the distance from the volcano.

On Fig. 3 this mode of transport for the distribution A is shown between four limits. The limit between suspended load and fallout is set at 4 phi and the particle size distribution of the tephra shown between this value and - 4 phi through - 1 phi (curves B-E). The tephra available for deposition changes its particle size distribution systematically towards better sorting as the interval between the suspended load and maximum particle size becomes narrower. Sheridan´s (1971) single energy environment of transport (fallout) describes the late stages of this process.

The particle size distribution of the Hekla 1970 tephra is obviously much coarser than the tephra represented by curve A, Fig. 3. Keeping in mind that the observed gradation between suspended load and fallout would stretch the fine tail of the computed distributions B-E towards the right it can be stated that the Hekla 1970 tephra was transported according to the simple model above with the suspended load/fallout limit between 5 and 6 phi.

It is concluded that although a sample of tephra is derived from the entire height of an eruption column its particle population never represents the population of the erupted material.

Two statements of fundamental importance in the studies of surface adsorbed compounds are summarized:

a) The particle size distribution of an eruption column is never represented by a single tephra sample since the ratio of coarse to fine particles decreases along the deposits.

b) The ratio of tephra deposited to total suspended load decreases drastically along the deposits.

Later in this text it will be shown that the chemistry of surface adsorbed material on tephra cannot be used as index of the overall chemistry of the volcanic gas phase (Rose, 1977) unless supported by a detailed knowledge of the particle size distribution of the erupted material and the samples studied.

LEACHING EXPERIMENTS AND MASS DISTRIBUTION OF SOLUBLE FLUORINE

Fluorine is known to be the principal toxic element associated with tephra (Stefánsson & Sigurjónsson, 1957; Sigurdsson & Pálsson, 1957).

Fluorine adsorbed on tephra is leached extremely fast by water. An example is the fluorine discharge of the small river Galtalækur draining an area covered by the 1970 tephra, west of Hekla. Fig. 5 shows that the fluorine content of the river increased by an order of magnitude for few hours following the eruption. The tephra was deposited in dry weather but on wet ground, at the end of the snow melting period, indicating that only contact between tephra and surface waters of the drained area is responsible for the fluorine pulse.

Numerous samples of tephra were leached in the laboratory following the eruption. Here only few well documented samples, collected during deposition, are discussed. The aim of the leaching experiments was to study the time needed to leach all water soluble fluorine and measure its quantity.

The results of the leaching experiments, shown in Tables II-V, can be summarized as follows:

a) The fluorine occurs in easily soluble form and is readily transferred to the aqueous phase (Talbe II).

b) The soluble fluorine is bound to the surface of the tephra particles. The amount of fluorine increases as the particle size decreases (Table III, curve D, Fig. 4).

c) The fraction of soluble fluorine increases along the AMT of the deposits as mean particle size decreases (Table IV, curve C, Fig. 2).

The estimated density distribution of soluble fluorine along the AMT is shown by curve E, Fig. 2. The discontinuity between $5 \cdot 10^4$ and $2 \cdot 10^5$ m is probably caused by the finer fractions of tephra from the smaller eruption column carrying down more fluorine. Curve E (kg/m^2) is combined with the mass distribution of the tephra to give curve D (kg/m), the mass distribution of soluble fluorine. The total mass of fluorine deposited is estimated from Curve D to be $3 \cdot 10^7$ kg. This value serves as minimum since the margins of the deposits are probably somewhat higher in fluorine due to higher fraction of fines. The total mass of the fines (suspended load) is, however, very small compared to the bulk of the tephra as indicated by the transversal density section on Fig. 2.

The density and mass distribution of soluble fluorine along the AMT reaches maximum some distance away from the volcano due to decreasing average particle size of the tephra. The density distribution of the soluble fluorine is sketched on Fig. 1. The lines of equal density are drawn to show the tendency towards a wider dispersion due to suspended load at the margins of the deposits.

It is evident from Fig. 2 that at very long distance away from the volcano the fluorine distribution curve E takes the shape of the density distribution for tephra curve A. Further it is clear that the velocity of the transporting medium and the height of the eruptive column determines the position of maximum fluorine density.

THE ADSORPTION OF FLUORINE ON TEPHRA

A leaching experiment on tephra is by no means the reverse of surface adsorption in the eruption column. Detailed analysis of leachate, shown in Table V, is, however, used to point out soluble chemical compounds which might be present on the surface of a fresh tephra particle. The high concentration of fluorine in the leachate explains the solubility of aluminium and silica, and high concentration of calcium indicate complexing of fluorine in the leachate. High amount of silica in weakly acid solutions favours presence of the fluosilicate anion. The excess acid of the leached compounds points towards a deliquescent mixture of solids adhering to the surface of the particles. This is in accordance with observations on volcanic fumes from Hawaii (Naughton et al., 1974)

A simple experiment was done to confirm the above assumptions. Constant amount of fume from the boiling azeotrop HF-H_2O was passed over washed and dryed tephra sample at temperatures between 1100 and 150°C. The tephra was then leached and the leachate analysed for fluorine. Above 700°C soluble fluorine was very low (80 ppm of the solid material) but increased lineary to 1500 ppm with decreasing temperature below 600°C. X-ray diffraction analysis show the high temperature fluorine compound to be calcium fluoride present in trace amounts but the low temperature compound is calciumfluosilicate (Fig. 6). This confirms that the chemistry of the leachate reflects the true composition of the adsorbed material.

Table V, column A, is the concentration of dissolved species in leachate, column B is the supposed ionic species and column C is the weight per cent of possible water soluble salts leached from the tephra. Calciumfluosilicate, the chlorides of calcium and sodium sodium fluoride and hydrochloric acid are the major components.

In order to visualize the soluble compounds, the tephra sample T04 was examined by SEM techniques. Plate Ia shows the surface of a broken tephra particle. No particulate matter adheres to its surface except small glassy fragments (marked A). The surface of the particle is, however, evenly etched (B on plate Ia) in contrast to the glassy fractured surface (C on plate Ia) and the walls of the vesicles inside the particle. This indicates that the soluble compounds were chemically adsorbed on the surface of tephra grains. To confirm this, tephra particles were mounted in epoxy and worked to a flat surface with diamond paste (water had to be avoided in the process) for compositional profiling.

Plate Ib shows the intensity of F k-alpha radiation along three profiles over the flattened top of a tephra particle. At points marked A, B, C and D, where the scanning profile crosses the surface boundary of the particle, fluorine is clearly visible, but not inside the vesicles as seen on points marked E and F.

The conclusion of this study is that the soluble compounds are chemically adsorbed on the surface of the tephra particles and that the reactions responsible for this are taking place in the cooling eruption column upon adsorption and condensation of the mineral acids of the gas phase.

NOTES ON REACTIONS AND ADSORPTION PROCESSES IN AN ERUPTION COLUMN

Degassing and cooling of extruded magma is an irreversible process. The gas phase separated attains equilibrium at atmospheric conditions by internal reactions and reactions with its surroundings of atmospheric air and silicate material.

Extremely variable conditions prevail in an eruption column. The temperature change from magmatic to ambient and proportions of tephra and gases change at variable air contamination.

The eruptive mechanism controlling particle size, thermal properties and dimensions of the eruption column can also change rapidly.

The acid magmatic gases SO_2, HCl and HF are the principal anion donors of water soluble compounds adhering to tephra. Their reactions in the eruption column can be resolved in the three temperature dependant reaction zones outlined below.

A) Salt formation zone

Microscopic salt particles are formed at magmatic temperatures during degassing of magma in the eruption vent and the hottest core of the eruption column.

Most likely to be formed are the chlorides, fluorides and sulfates of the alkali metals and calcium (Naughton et al., 1974) and the formation of sulfates favoured by an oxidizing environment. Although a small fraction of the total production of a volcano, these particles are likely to be detected long distances away from it, since they are supposedly transported as suspended load.

B) Surface adsorption zone

At intermediate temperatures (below 700°C) the halogene acid gases react with solidified silicate material by surface adsorption. The rate of adsorption increases with falling temperatures. Hydrochloric acid is probably adsorbed preferentially at higher temperatures but hydrofluoric acid at lower temperatures.

C) Condensation zone

At temperatures below 338°C sulfuric acid condensates as aerosol. The rate of formation depends on oxidation of sulfur dioxide by atmospheric oxygen:

$SO_{2(g)} + 1/2\ O_{2(g)} \rightarrow SO_{3(g)}$ $SO_{3(g)} + H_2O_{(g)} \rightarrow H_2SO_{4(1)}$

Below 120°C the halogene acid water azeotrops condensate. Halogene acid aerosols are thus formed prior to the condensation of water.

All the acid aerosols adsorb water vapour upon cooling and if, at reducing conditions, sulfur dioxide still remains in the gas phase it will be adsorbed in diluted acids and water. The sulphite formed will later be oxidized to sulfate by atmospheric oxygen or ferric iron on particle surfaces.

On Fig. 7 the hypothetical shape and thermal properties of a plinian eruption column are outlined. The shape of the reaction zones mentioned above is indicated by isotherms. These are suppressed to the lower region of the transportation zone due to the large heat content of the fallout. The paths of tephra particles are indicated by dashed lines to show the separation of suspended load (marked by S in Fig. 7) and fallout (marked by F in Fig. 7).

Continuous gradation between the reaction zones is maintained by transportation of all material from an inner zone through the outer zones.

Mixing with atmospheric air and oxidation occur more readily at the upwind side of the column. Oxidized material is transported downwind and mixed with the inner core of the column. The velocity of the transporting medium thus greatly influence the overall oxidation state of the column. The transportation zone marked in Fig. 7 contains most of the suspended load and gases of the eruption column. As the distance from the volcano increases the fallout is shown to separate from the suspended load and gases.

Separation processes of acid gases and their reaction products are likely to be active in all eruption columns. The salt particles formed in zone A and acid aerosols formed in zone C (Fig. 7) separate from the fallout under transport. The halogenes adsorbed in zone B are carried down with the fallout and their proportions in the gas phase (supposedly) change due to different adsorption affinity of HCl and HF.

In zone C condensation of the acid vapours and water can take place on the surface of tephra particles. Since the largest particles cool slower than the suspended load, condensation takes place on the smallest particles, again leading to separation of the acids and tephra.

The separation of the halogenes is evident from Table III. The Cl and F (curve D, Fig. 4) concentrations in leachate of particle size fractions increases with decreasing particle diameter. The Cl/F ratio shown by curve E Fig. 4, changes drastically in the observed particle size region. An explanation of this is shown on Fig. 7. At a sampling site marked L the maximum, mean and minimum particles sizes are derived from three various regions in the eruption column. The variation of the Cl/F ratio of the particle fractions (curve E, Fig. 4) indicate that fluorine is adsorbed at the highest rate on the medium sized particles, reflecting their transport from the intermediate temperature zone (B) of the column.

Since the eruption mechanism responsible for the physical properties of an eruption column is a major factor controlling the chemistry of soluble compounds of the tephra, each eruption type is supposedly characterized by some dominating mode of origin for the soluble compounds.

In a plinian column tephra and the volcanic gas phase are intimately mixed for a relatively long time. All the above mentioned processes can thus be expected to be active and a relatively large fraction of the volatiles will be carried down by the tephra.

Strombolian activity characterized by columns of short duration (Blackburn et al., 1976) greatly minimize the time available for the low temperature processes.

In lava fountaining activity most of the volatiles separated from the magma are released to the atmosphere, due to limited possibilities of gas solid reactions in the small and hot eruption column.

The potential hazard associated with toxic elements produced in a volcanic eruption depends on the eruption type. Comparing the plinian and fountaining activity, the former spread the toxic compounds over a defined area in a short time, while the later produces these compounds at a defined location without controlling their distribution. The potential hazard of toxic compounds from fountaining activity thus increases directly with size and duration of the eruption.

SUMMARY

The factors governing deposition and particle size distribution of tephra are evaluated by the aid of observations on the Hekla 1970 tephra. In was concluded that a tephra sample is not representing the particle population of the erupted material. Leaching experiments and SEM studies show the water soluble fluorine to be chemically adsorbed on the surface of the tephra particles.

Factors governing reactions between volcanic gas and solid tephra in the eruption column are evaluated. Three reaction types, salt formation, adsorption and condensation are resolved and their action in various eruption types outlined. It is concluded that the chemistry of water soluble compounds adhering to tephra reflects the origin of the tephra samples within the eruption column as well as the composition of the volcanic gas phase.

REFERENCES

Blackburn, E.A. et al., 1976. Mechanism and dynamics of strombolian activity. J. Geol. Soc. 132, 429-440.

Naughton, J.J. et al., 1974. The chemistry of sublimates collected directly from lava fountains of Kilauea Volcano, Hawaii. Geochim. Cosmochim. Acta 38, 1679-1690.

Rose, W.I. Jr., 1977. Scavenging of volcanic aerosol by ash: Atmospheric and volcanologic implications. Geology 5, 621-624.

Sigurdsson, B. & Pálsson, P.A., 1957. Fluorosis of Farm Animals During the Hekla eruption of 1947-1948. Pp. 1-12 in The Eruption of Hekla 1947-1948, III, 3. Soc. Sci. Islandica, Reykjavik.

Sigvaldason, G.E., 1974. The petrology of Hekla and origin of silicic rocks in Iceland. Pp. 1-44 in The Eruption of Hekla 1947-1948, V, 1. Soc. Sci. Islandica, Reykjavik.

Sheridan, M.F., 1971. Particle-Size Characteristics of Pyroclastic Tuffs. J. Geophys. Res. 76, 5627-5634.

Sparks, R.S.J. & Wilson, L., 1976. A model for the formation of ignimbrite by gravitational column collapse. J. Geol. Soc. 132, 441-451.

Stefánsson, K. & Sigurjónsson, J., 1957. Temporary Increase in Fluorine Content of Water Following the Eruption. Pp. 1-13 in The Eruption of Hekla 1947-1948, III, 2. Soc. Sci. Islandica, Reykjavik.

Thorarinsson, S., 1967. The Eruptions of Hekla in Historical Times. Pp. 1-170 in The Eruption of Hekla 1947-1948, I. Soc. Sci. Islandica, Reykjavik.

Thorarinsson, S., 1970: Hekla. A Notorious Volcano. Almenna Bókafélagid, Reykjavik. 61 p.

Thorarinsson, S. & Sigvaldason, G.E., 1972. The Hekla Eruption of 1970. Bull. Volc. 36, 269-288.

Walker, G.P.L. et al., 1971. Explosive Volcanic Eruptions - I. The Rate of Fall of Pyroclasts. Geophys. J. R. astr. Soc. 22, 377-383.

Wilson, L., 1976. Explosive Volcanic Eruptions - III. Plinian Eruption Columns. Geophys. J. R. astr. Soc. 45, 543-556.

TABLE I

Computed max. and mean elevation of tephra samples

Sample	Distance	Max.elev.	Mean elev.
T00	16 km	16.9 km	8.1 km
T04	36 -	9.1 -	3.0 -
T23	187 -	15.4 -	10.0 -
T21	215 -	12.5 -	8.3 -
Average		13.5 km	7.4 km

TABLE II (ppm of leached tephra)

Analysis of leachate of sample H´70 T23

min.	F	Cl	Na^+	Ca^{2+}
0	650	825	350	500
7.5	850	1400	380	530
15	1000	1510	390	530
30	1000	1590	390	530
60	1000	1650	390	530
120	1000	1650	400	530
240	1000	1680	410	530
300	1100	1680	430	530

A plastic bottle containing 100 ml. distillated water and 2000 mg sample was shaken on a machine for 0-300 min. The leachate was filtered through Wathman 42 paper and analysed. The results are reported as ppm of the solid tephra.

TABLE III (ppm of leached tephra)

Leachate of particle size fractions of the sample H´70 T04

d(mm)	F^-	Cl^-	Na^+	K^+	Ca^{2+}	Mg^{2+}	Cl/F
0.500	375	825	225	162	210	12.5	2.2
0.250	500	880	200	36	225	14.0	1.8
0.125	625	910	300	26	260	11.0	1.5
0.063	1000	1180	410	45	500	9.0	1.2
0.040	1250	1590	525	60	890	8.5	1.3
0.040	1500	2760	575	62	825	8.5	1.8

A plastic bottle containing 2000 mg of sample and 100 ml distillated water was shaken on a machine for one (1) hour. The leachate was filtered through Wathman 42 paper and analysed.

TABLE IV (ppm of leached tephra)

Sample	F	Cl	SO_4^{2-}	Na^+	K^+	Ca^{2+}	Mg^{2+}
H´70 T00	375	310	72	63	24	100	3.0
H´70 T04	750	1500	63	350	70	375	19.0
H´70 T23	1000	1300	156	390	50	475	27.0
H´70 T31	1000	1050	205	451	70	475	17.0

Procedure the same as describe below table II.

TABLE V

Composition of leachate from sample H´70 T04a

	A ppm		B meq		C %
F	188	F	1.21	NaF	6.5
Cl	245	Cl	6.91	HCl	11.7
SO_4^{2-}	16	SO^{2-}	0.33	$MgSO_4$	3.0
Na^+	81	Na^+	3.52	NaCl	19.4
K^+	17	K^+	0.43	KCl	4.6
Mg^{2+}	4.8	Mg^{2+}	0.40	$MgCl_2$	0.4
Ca^{2+}	96	Ca^{2+}	4.79	$CaCl_2$	16.0
SiO_2	84	SiF_6^{2-}	2.80	$CaSiF_6$	36.7
Al^{+3}	3.9	AlF_2^+	0.14	AlF_3	1.7
H^+	pH 2.65	H^+	2.24		
		Balance	+.27	Sum	100.0

A) The sample (100 g) is shaked with (400 ml) distillated water for one hour. The column shows analysis of the leachate.

B) The values from A are converted to contain the fluosilicate anion and aluminium di-fluoride ion and the charge balance computed.

C) Species from B converted to soluable solid compounds and hydrochloric acid and reported as weight per cent of solid (deliquescent) material.

TEXT TO FIGURES AND PLATES

Fig. 1. The tephra deposits of the 1970 Hekla eruption. The lines show the density of soluble fluorine (10^{-2} kg/m^2) and the dashed lines show density of the tephra deposits (kg/m^2). Dotted lines show the margins of the deposits (Thorarinsson, 1970). Filled circles show sampling localities. The samples discussed in the text are marked on the figure.

Fig. 2. Distribution patterns along the tephra deposits. The horizontal scale is distance from the volcano. The curves are indexed with letters to show their scale on the ordinate.

A: Density of tephra (kg/m^2) along the AMT.
B: Mass distribution of tephra (10^3 kg/m) along the AMT.
C: Concentration of soluble fluorine along the deposits (ppm).
D: Mass distribution of suluble fluorine along the deposits (kg/m).
E: Density distribution of soluble fluorine along the AMT (10^{-5} kg/m^2).
F: Density sections (kg/m^2) across the deposits along the AMT. The sections are drawn with the 250 km as a central line (AMT). The scale of the sections is that of curve A five times enlarged. The distance from the volcano is marked on the sections.

Fig. 3. Particle size distribution of the Hekla 1970 tephra. Cumulative curves are plotted on probability scale vs. phi-value. Sample locations are shown on Fig. 1. Curve A is cumulative particle size distribution of a plinian eruption column (Sparks & Wilson, 1976) and curves B-E represent distributions derived from A by selective transport of particles between a fixed size (4 phi) and a variable limit ÷4 to ÷1 phi.

Fig. 4. Curves A and B show mean and maximum particle size of the tephra as the phi-value (right ordinate) plotted against distance from the volcano (lower abscissa). Curve C shows the density (10^3 kg/m^3) of tephra samples (left ordinate) as a function of distance. Curve D shows soluble fluorine as ppm of the tephra (upper abscissa) as a function of the Phi-values of the fractionated sample T04 (ref. Table III). Curve E shows the Cl/F ratio of the leachates of the fractionated sample T04 (upper abscissa), plotted against the phi-value.

Fig. 5. Fluorine in the river Galtalækur as a function of time following the Hekla 1970 eruption.

Fig. 6. Absorption of HF on tephra from the Hekla 1970 eruption. One ml of the gaseous HF-H_2O azeotrope was passed over 2 grms of washed and dryed tephra at various temperatures using carbon dioxide as a carrier. The soluble fluorine is reported as ppm of the tephra.

Fig. 7. Hypothetical shape and thermal properties of a plinian eruption column. The zones A, B and C refer to reaction zones discussed in the text. The dashed lines within the column represent paths of tephra particles showing the separation of suspended load (S) and fallout (F).

Plate Ia. SEM-photograph of tephra particle from the sample T04.

Plate Ib. Profiles of F-K_{alpha} radiation over the flattened surface of tephra particle. Feldspar lath is visible in the upper middle of the photograph.

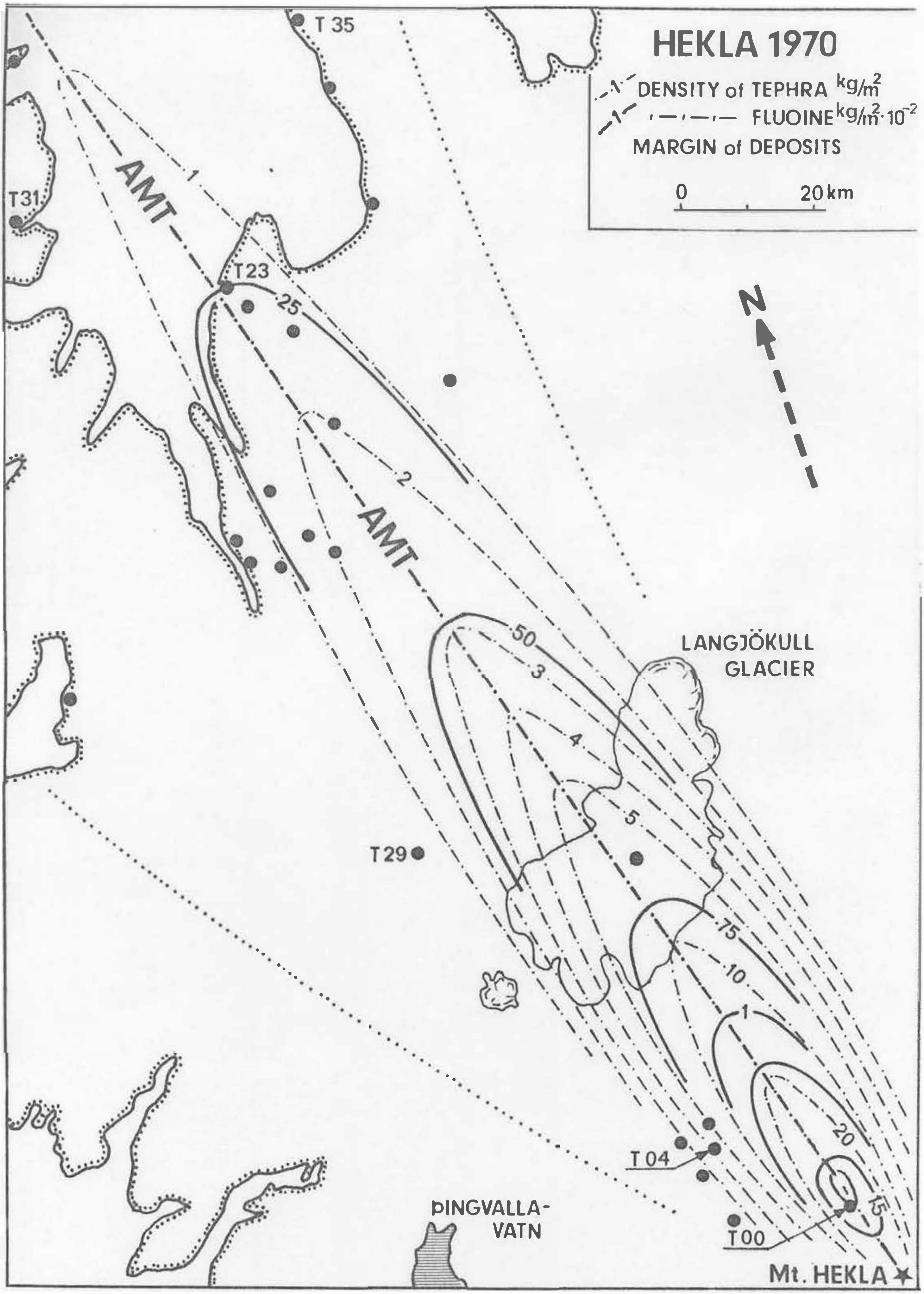
HEKLA 1970
1 DENSITY of TEPHRA kg/m2
1 FLUOINE kg/m2·10-2
MARGIN of DEPOSITS
0
20 km
N
T 35
T31
AMT
1
T23
25
2
AMT
50
3
4
5
LANGJÖKULL
GLACIER
T29
7.5
10
1
20
15
T 04
T 00
ÞINGVALLA-
VATN
Mt. HEKLA

FIG1

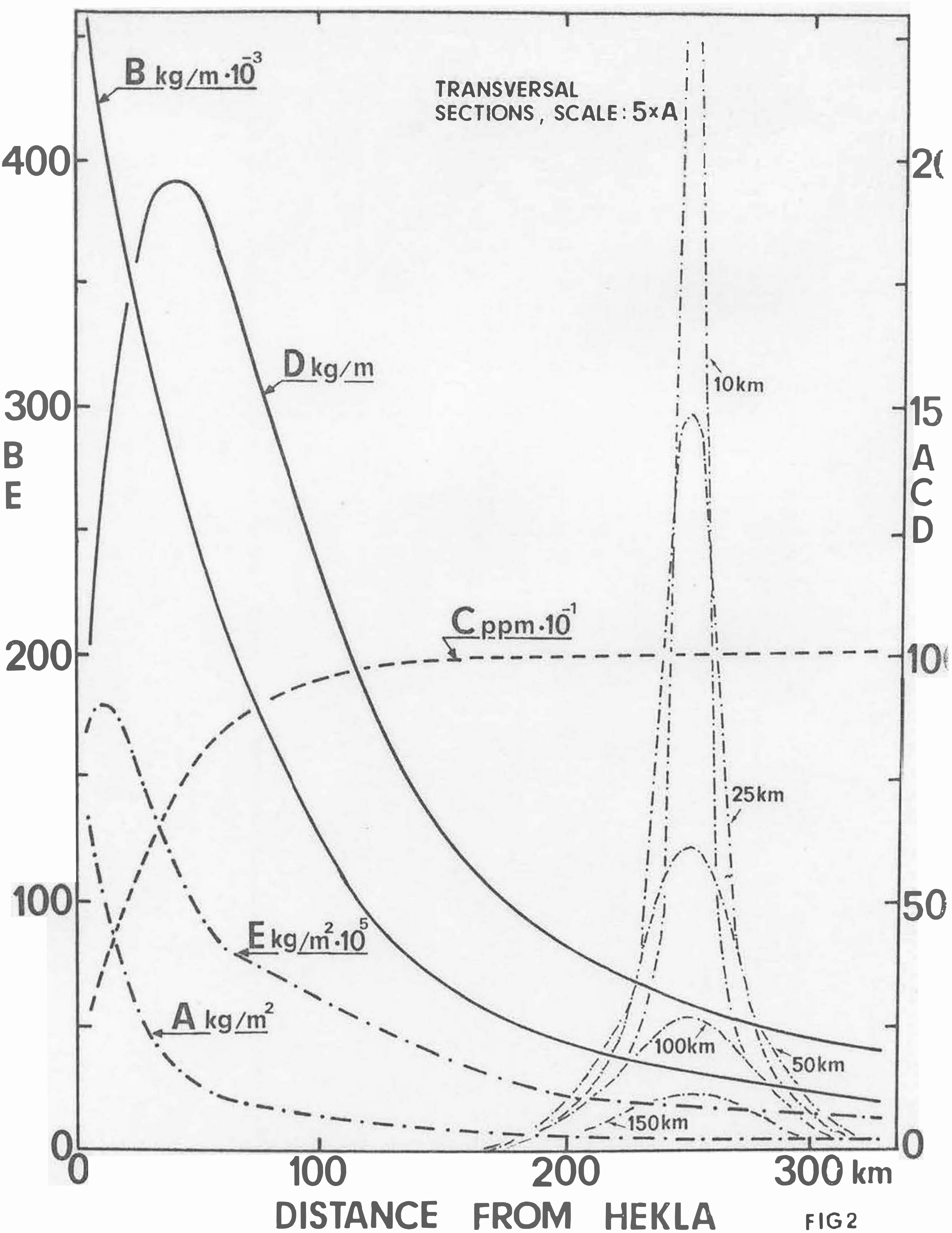
B kg/m·10⁻³
TRANSVERSAL SECTIONS, SCALE: 5×A
D kg/m
10km
25km
C ppm·10⁻¹
E kg/m²·10⁵
A kg/m²
100km
50km
150km
400
300
200
100
0
B
E
20
15
10
50
0
A
C
D
0
100
200
300 km
DISTANCE FROM HEKLA

FIG 2

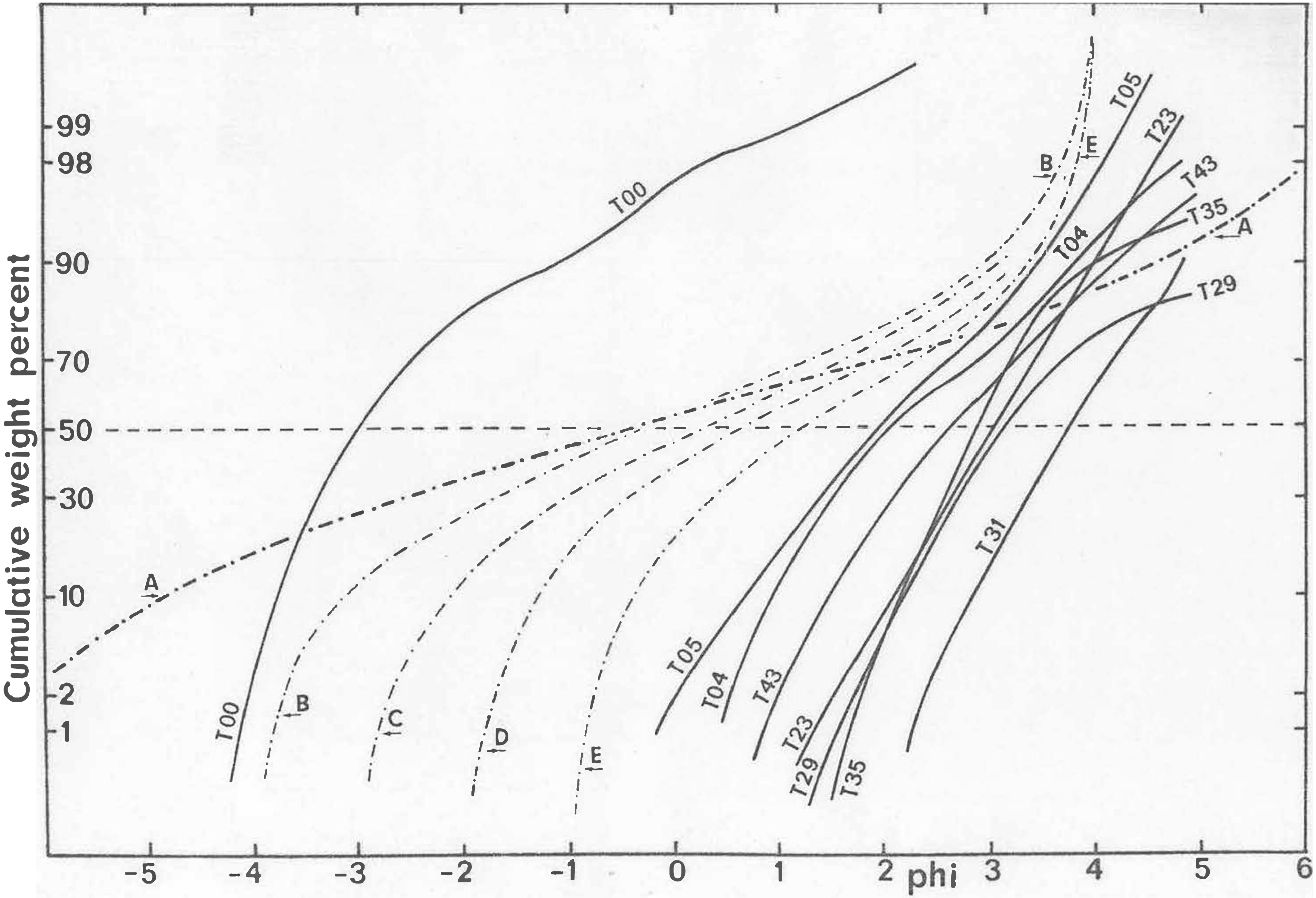
Cumulative weight percent
1
2
10
30
50
70
90
98
99
phi
-5
-4
-3
-2
-1
0
1
2
3
4
5
6
T00
T05
T04
T43
T23
T29
T35
T31
A
B
C
D
E

FIG 3

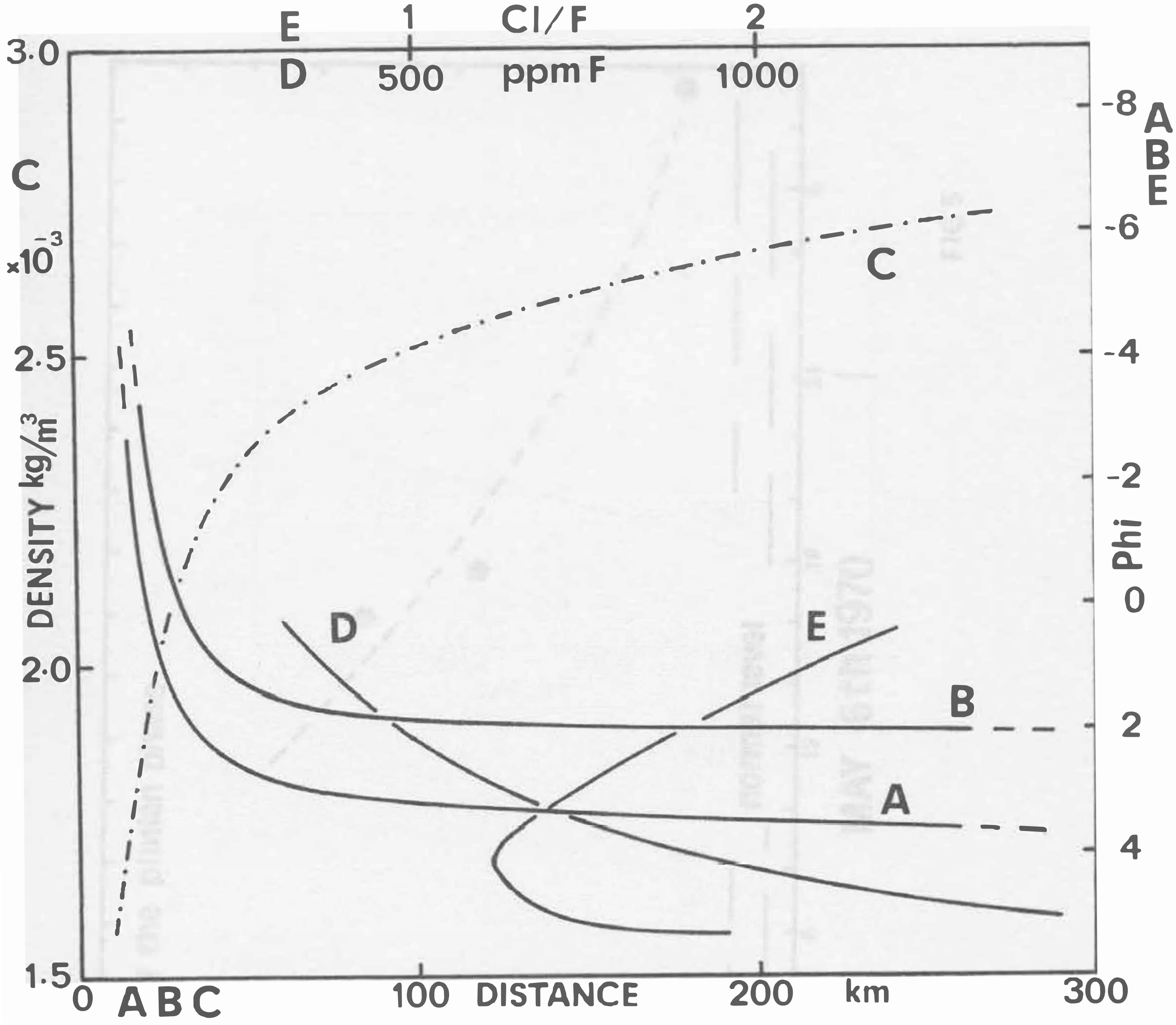
E
1
Cl/F
2
D
500
ppm F
1000
3·0
C
×10⁻³
2.5
DENSITY kg/m³
2·0
1.5
0
A B C
100
DISTANCE
200
km
300
-8
A
B
E
-6
-4
-2
Phi
0
2
4
C
D
E
B
A

FIG 4

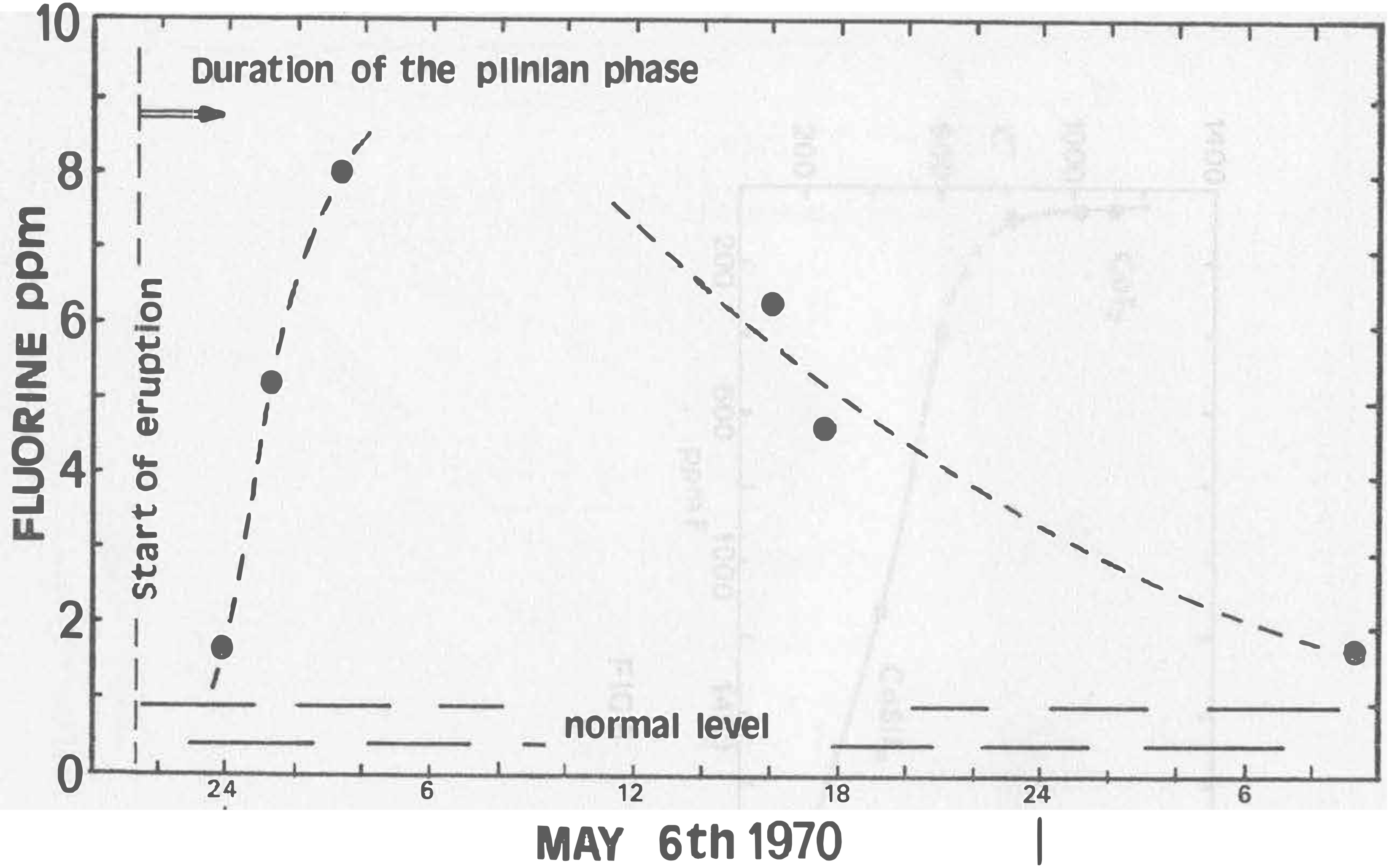
10
8
6
4
2
0
FLUORINE ppm
Start of eruption
Duration of the plinian phase
normal level
24
6
12
18
24
6
MAY 6th 1970

FIG 5

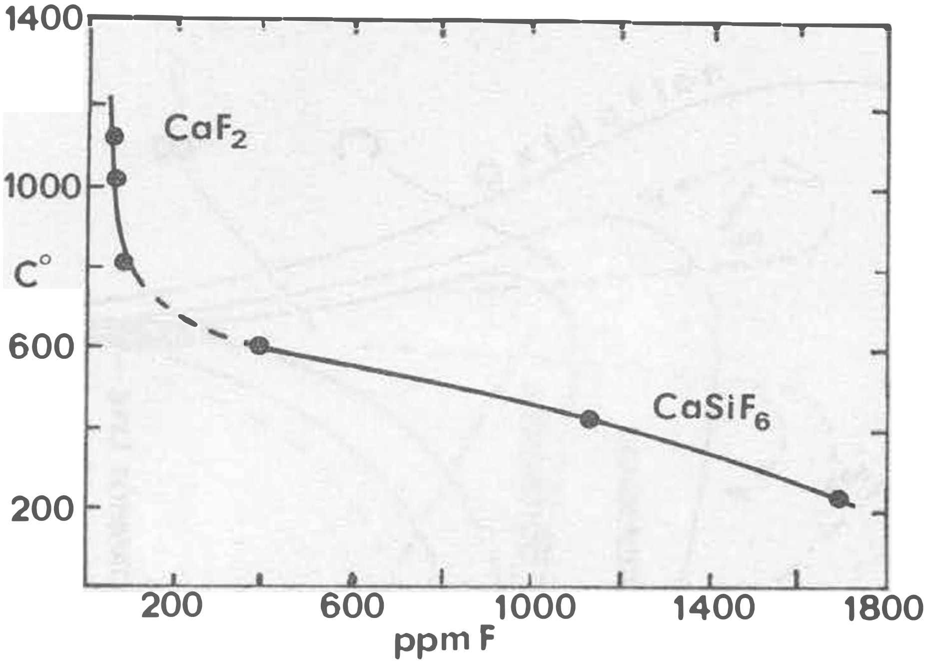

FIG 6

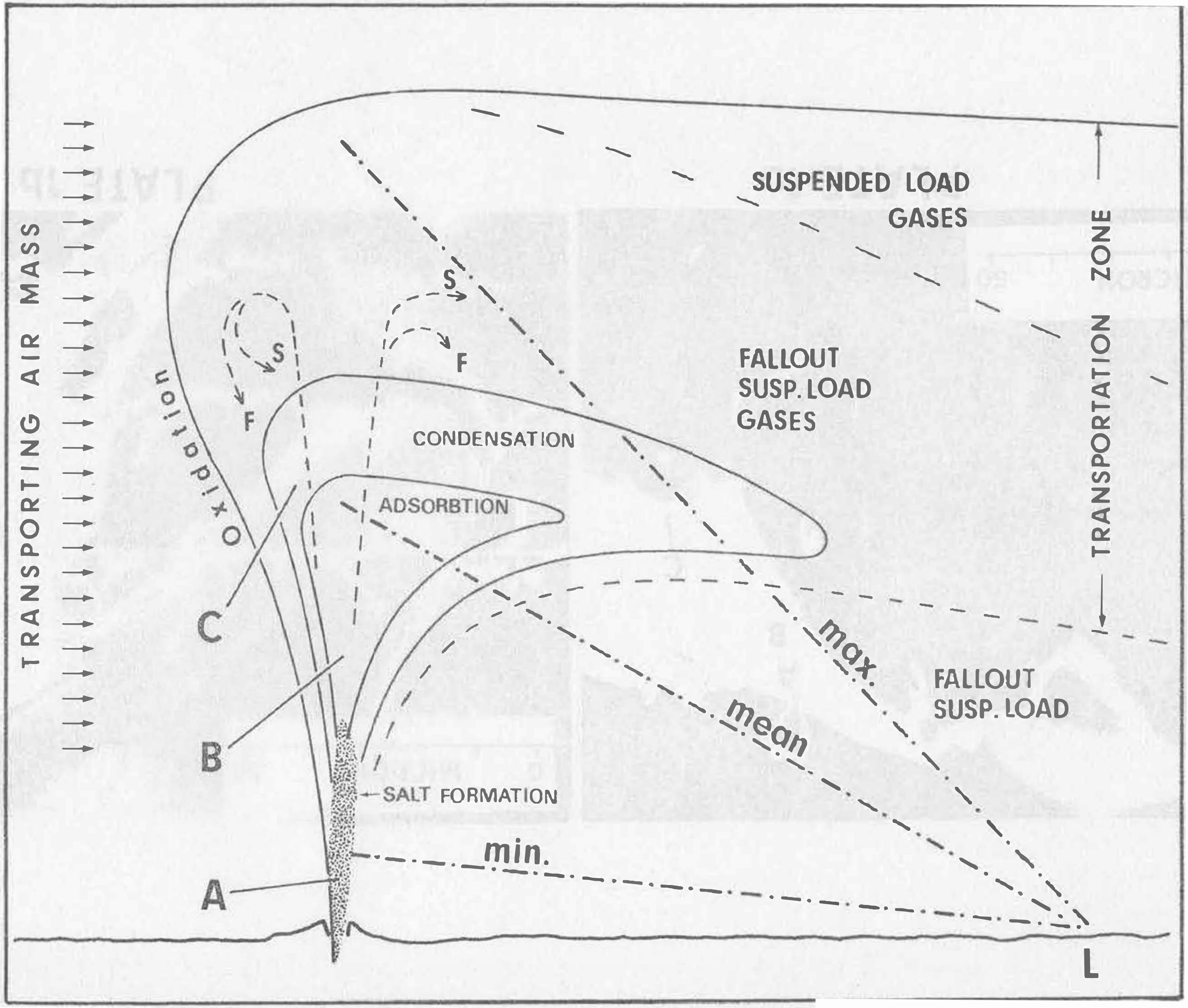
TRANSPORTING AIR MASS
Oxidation
S
F
S
F
CONDENSATION
ADSORBTION
C
B
A
SALT FORMATION
min.
mean
max.
SUSPENDED LOAD
GASES
FALLOUT
SUSP. LOAD
GASES
FALLOUT
SUSP. LOAD
TRANSPORTATION ZONE
L

FIG 7

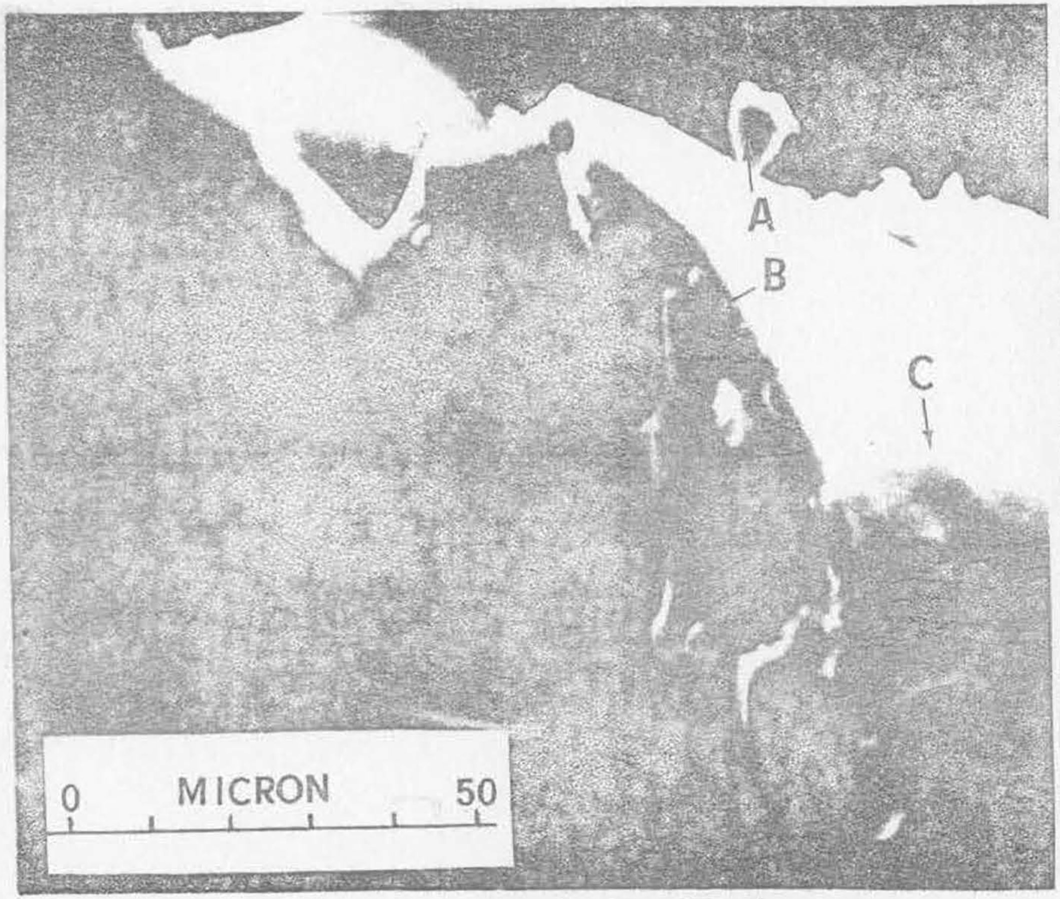

PLATE 1a

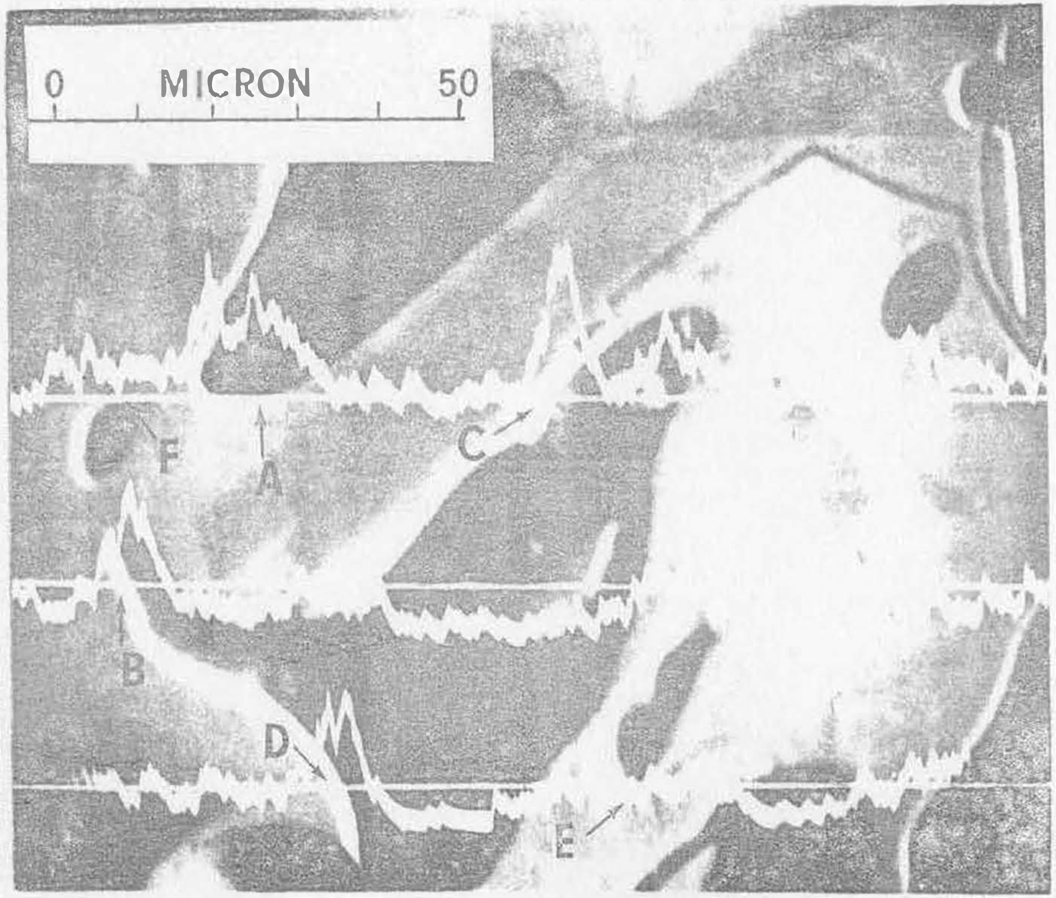

PLATE 1b